Struct Multidisc Optim (2012) 46:425–444
DOI 10.1007/s00158-012-0771-y

INDUSTRIAL APPLICATION

Robust springback optimization of a dual phase steel seven-flange die assembly

Deniz Bekar · Erdem Acar · Firat Ozer · Mehmet Ali Guler

Received: 28 September 2011 / Revised: 5 January 2012 / Accepted: 10 January 2012 / Published online: 31 January 2012

Abstract This paper investigates robust springback optimization of a DP600 dual phase steel seven-flange die assembly composed of different flange designs. The optimum values of the die radius and the punch radius are sought to minimize the mean and the standard deviation of springback using surrogate based optimization. Springback values at the training points of surrogate models are evaluated using the finite element analysis code LS-DYNA. In this work, four different surrogate modeling types are considered: polynomial response surfaces (PRS) approximations, stepwise regression (SWR), radial basis functions (RBF) and Kriging (KR). Two sets of surrogate models are constructed in this study. The first set is constructed to relate the springback to the design variables as well as the random variables. It is found for the first set of surrogate models that KR provides more accurate springback predictions than PRS, SWR and RBF. The mean and the standard deviation of springback are calculated using Monte Carlo simulations, where the first set of surrogate models is utilized. The second set of surrogate models is generated to relate the mean and the standard deviation of springback to the design variables. It is found for the second set of surrogate models that PRS provides more accurate springback predictions than SWR, RBF and KR. It is also found that introducing beads increases the mean performance and the robustness. The robust optimization is performed and significant springback reductions are obtained for all flanges ranging between 7% and 85% compared to the nominal design. It is also found that a design change that decreases the mean springback also reduces the springback variation. It is observed that the optimization results heavily dependent on the bounds of the die and punch radii. In addition, optimization with multiple surrogates is investigated. Finding multiple candidates of optimum with multiple surrogates and selecting the one with the best actual performance is found to be a better strategy than optimizing using the most accurate surrogate model.

Keywords Dual phase steels · Finite element analysis · Monte Carlo simulations · Springback · Surrogate models · Robust optimization

D. Bekar · E. Acar (✉) · F. Ozer · M. A. Guler
Department of Mechanical Engineering,
TOBB University of Economics and Technology, Sogutozu Cad.
No: 43, Sogutozu, Ankara, 06560 Turkey
e-mail: acar@etu.edu.tr

D. Bekar
e-mail: dbekar@etu.edu.tr

F. Ozer
e-mail: fozer@etu.edu.tr

M. A. Guler
e-mail: mguler@etu.edu.tr

1 Introduction

Automotive industry has increased the use of high strength dual phase (DP) steels as an alternative to aluminum and magnesium alloys due to their light weight, low cost and durability. An important issue related to the dual phase steels is springback. Springback is observed during sheet metal forming process and defined as the deviation of the manufactured geometry from the designed geometry. Furthermore, springback variation is another difficult problem to overcome. Large variation in springback limits the application of springback prediction and compensation

techniques. Uncertainties in mechanical and geometrical properties of the material and the process parameters are the main reasons for springback variation. Accurate determination of the uncertainties in material properties and forming process parameters provides reliable results and improves the final product quality. Therefore, performing a robust optimization study is a must. A design is called robust if it is insensitive to the uncertainties. The aim of a robust optimization study is to obtain maximum average performance with minimum performance variation in the presence of uncertainties.

The main challenge in a springback optimization study (either a deterministic optimization study or a robust optimization study) is the requirement to perform computationally expensive forming analyses through finite element method. The most popular remedy to alleviate this problem is to utilize surrogate models that can mimic the results of finite element analyses. The examples of surrogate-based deterministic springback optimization studies are the followings. Naceur et al. (2006, 2008) and Wei et al. (2009) applied the integration between finite element methods (FEM) and polynomial response surface approximations (PRS) to find out both material and process parameters for springback minimization. Other than PRS, other surrogate modeling techniques such as Kriging (Strano 2008) and neural networks (Liew et al. 2004) are also utilized for springback prediction.

The examples of surrogate-based robust springback optimization studies are the followings. Wang et al. (2009) investigated a systematic and robust approach, gathering the FEM (finite element method) and stochastic statistics to decrease the sensitivity of high strength steel (HSS) stamping in the presence of uncertainties. They applied a separate interval adaptive response surface methodology in modeling sheet metal stamping. Also, they employed Monte Carlo simulations (MCS) to simulate the stochastic response of material/process variations to stamping quality and to provide optimal designs to reduce the sensitivity of process uncertainties. They only focused on formability of HSS. Li et al. (2005) applied a computer aided engineering (CAE)-based six sigma robust design for sheet metal forming process. They integrated statistical technology and dual response surface approximate model together to perform reliability optimization and robust improvement. They investigated a deep drawing process to illustrate their method. Zhang and Shivpuri (2008) investigated the reliability of optimal blank holder force (BHF) in the presence of process uncertainties by minimizing the magnitude of wrinkling and fracture defects under probabilistic constraints. They developed a response surface approximate model and used it in the probabilistic optimization. They analyzed a conical cup drawing of aluminum killed deep-drawing quality steel under process uncertainties. Du et al. (2009) studied the robustness and robust mechanism synthesis when random and interval variables are involved. When the robustness is properly ensured and the minimization of performance variations are obtained, robust design leads to desired results without much performance variation due to uncertainties.

The springback optimization studies in metal forming of sheets made of conventional steel are well established. The optimization studies on DP steels, on the other hand, have started in the last years. Meinders et al. (2008) performed deterministic springback optimization of DP965 steels using FEM and surrogate modeling techniques. They used sequential approximate optimization algorithm, where the accuracy of surrogate models are improved sequentially until convergence during optimization. Ingarao et al. (2009) investigated deterministic springback minimization problem through integration between numerical simulations, response surface methodology (RSM) and Pareto optimal solutions search techniques. They examined the design of a U-channel stamping operation utilizing two different DP steels, DP1000 and DP600. They optimized friction conditions and BHF as design variables in order to reduce excessive thinning and avoid excessive geometrical distortions due to springback occurrence. Marretta et al. (2010) investigated an S-shaped U-channel stamping operation carried out on a lightweight aluminum alloy. They developed a design tool for the prevention of excessive part thinning and the control of springback phenomena. They proposed a multi-objective optimization problem consisting of integration among FEM numerical simulation, RSM and MCS method to deal with sheet stamping process variability.

There exist uncertainty analyses of springback of DP steels in literature (Chen and Koc 2007; de Souza and Rolfe 2010); however, robust springback optimization has not been investigated yet. The main academic contribution of the present paper aims to fill this gap, while the industrial contribution of the paper is explained in the next paragraph.

COŞKUNÖZ METAL FORM Company is a leading die manufacturer supplying automotive parts for the original equipment manufacturers (OEMs) such as Ford Otosan, Mercedes, Renault, Tofaş-Fiat, etc. The company works with quite a few different material suppliers including domestic and international counterparts. This leads to a significant variation of the material properties. The major difficulty faced by the die engineers in COŞKUNÖZ is to manufacture parts within a certain tolerance requested by the OEMs. COŞKUNÖZ discovered that the variability of mechanical properties results in a significant variation in the springback behavior over different manufactured parts. The variation of springback over different manufactured parts restricts the use of springback compensation

Table 1 The features of each flange

Flange #	1	2	3	4	5	6	7
Die radius (mm)	3	7	7	5	7	10	5
Punch radius (mm)	5	7	7	5	7	–	5
Bend angle (deg)	110	90	90	105	100	90	100
Flange type	WFO	SHF	STF	WFO	WFO	SF	WFO
Stroke (mm)	40	40	40	40	40	35	40
Bead	Yes	–	–	Yes	–	–	–

measures. COŞKUNÖZ has decided to conduct a research with the authors as part of a university-industry collaboration about predicting the springback behavior of several flange types that can be often encountered in the automotive industry. COŞKUNÖZ engineers and the authors designed a seven-flange die assembly for that purpose based on their experiences. Robust springback optimization of the seven-flange die assembly is performed in this study. It should be noted here that the seven-flange die assembly is designed for research purpose, it is not an actual end product. However, it gives great insights about the springback behavior of different flange design types that could be used by a die design engineer. The methodology developed will be used to improve design guidelines of the die design group at COŞKUNÖZ. Die design is an iterative procedure. The methodology developed can help to reduce the number of iterations to achieve their final product.

In this paper, four different surrogate modeling types, namely PRS (Myers and Montgomery 2002), stepwise regression (SWR; Myers and Montgomery 2002), radial basis functions (RBF; Buhmann 2003) and Kriging (KR; Sacks et al. 1989; Lophaven et al. 2002), are constructed for finite element analysis (FEA) springback prediction, and the most accurate model is used in the robust optimization study. Therefore, we determined the most suitable surrogate model for springback behavior of each flange. This approach provides more reliable results other than utilizing one surrogate model through prediction and optimization process. Springback values at the training points of surrogate models are evaluated using a coupled explicit-implicit solving algorithm (Finn et al. 1995).

The paper is organized as follows. The next section provides the problem description of the robust springback optimization of the seven-flange die assembly composed of different flange designs. Section 3 presents the details of the FEA of the forming process of the flanges. Section 4 discusses surrogate model construction and provides the accuracies of the first set of surrogate models. Section 5 explains the optimization methodology followed and discusses the second set of surrogate models. The results of the optimization problems are given in Section 6, followed by concluding remarks given in Section 7.

2 Problem description

The design is composed of seven typical flange conditions which includes a straight flange (SF, Flange #6), four wipe flanges with outflanges (WFO, Flanges #1, 4, 5, 7), two flanges contained stiffening beads or darts to reduce overall springback, a stretch flange (STF, Flange #3), a shrink flange (SHF, Flange #2) and various flange radii. Table 1 provides an overview of the features for each flange.

Numbering of the flanges is shown in Figs. 1 and 2. The flanges should be designed for minimum mean and standard deviation of springback which is defined by two angles (θ_1 and θ_2). In order to determine the springback angles after the forming process and to compare the FEA results to the experiments, a measurement procedure given in Fig. 3 has been developed. Thereby, the measurement consistency between the FEA results has been guaranteed.

For each flange, two angles have been measured between the surfaces A–B and B–C. Then the averages of these angles have been used to obtain the springback angles θ_1 and θ_2 as given in (1).

$$\theta_i = \theta_{target} - (\text{Angle between the surfaces})_{average} \quad (1)$$

The variables of the problem are divided into two groups. The first group consists of two design variables; (i) the die radius, R_d; (ii) the punch radius, R_p. The second group consists of seven random variables; (i) the yield stress, σ_y; (ii) the hardening exponent, n; (iii) the hardening coefficient,

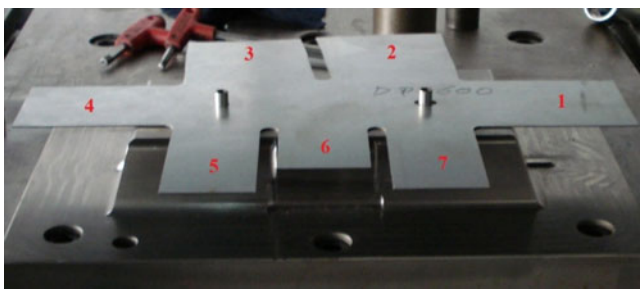

Fig. 1 Appearance of the flanges before the forming process

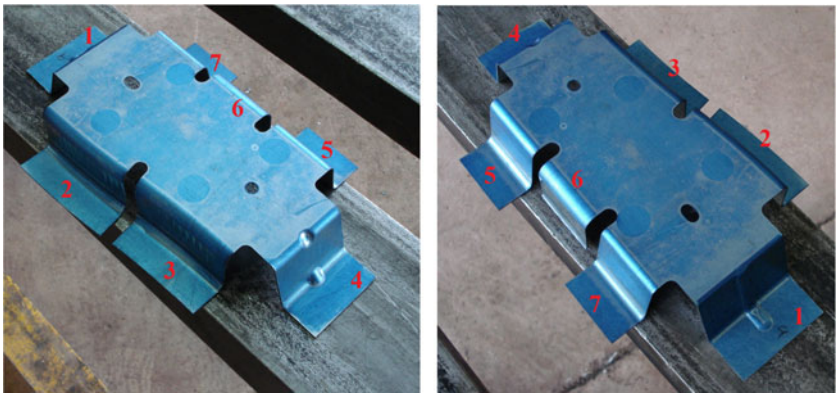

Fig. 2 Appearance of the flanges after the forming process

K; (iv–vi) the anisotropy coefficients, R_0, R_{45}, R_{90}; and (vii) the rolling direction, RD. The random variables are selected by the authors and the die engineers of the COŞKUNÖZ Company. Commonly used noise variables in the literature are used.

COŞKUNÖZ die engineers mentioned that the human error is one of the main reasons for uncertainty. Sometimes a lousy worker does not pay attention to the rolling direction. So we ended up having the rolling direction as a random variable. The chance of using the true rolling direction is taken as 50%, and this is a large probability. However, it can be considered that all human errors (e.g., errors in tests, interpretation of test results) are boiled down to a single random variable.

In this study, three different optimization cases are considered for each flange (except Flange #6, there is only a single case). The first case is the minimization of both the mean and the standard deviation of θ_1, second case is the minimization of both the mean and standard deviation of θ_2, and the last case is the minimization of both the mean and standard deviation of $\theta_1 + \theta_2$. For Flange #6, only optimization of θ_1 is considered. The robust optimization problems can be formulated as given in (2–4).

$$\begin{aligned} &find && R_d, R_p \\ &\min && w_1 \frac{\mu_{\theta_1}(R_d,R_p)}{\mu_{\bar{\theta}_1}} + w_2 \frac{\sigma_{\theta_1}(R_d,R_p)}{\sigma_{\bar{\theta}_1}} \\ &s.t && R_d^L \le R_d \le R_d^U \\ & && R_p^L \le R_p \le R_p^U \end{aligned} \tag{2}$$

$$\begin{aligned} &find && R_d, R_p \\ &\min && w_1 \frac{\mu_{\theta_2}(R_d,R_p)}{\mu_{\bar{\theta}_2}} + w_2 \frac{\sigma_{\theta_2}(R_d,R_p)}{\sigma_{\bar{\theta}_2}} \\ &s.t && R_d^L \le R_d \le R_d^U \\ & && R_p^L \le R_p \le R_p^U \end{aligned} \tag{3}$$

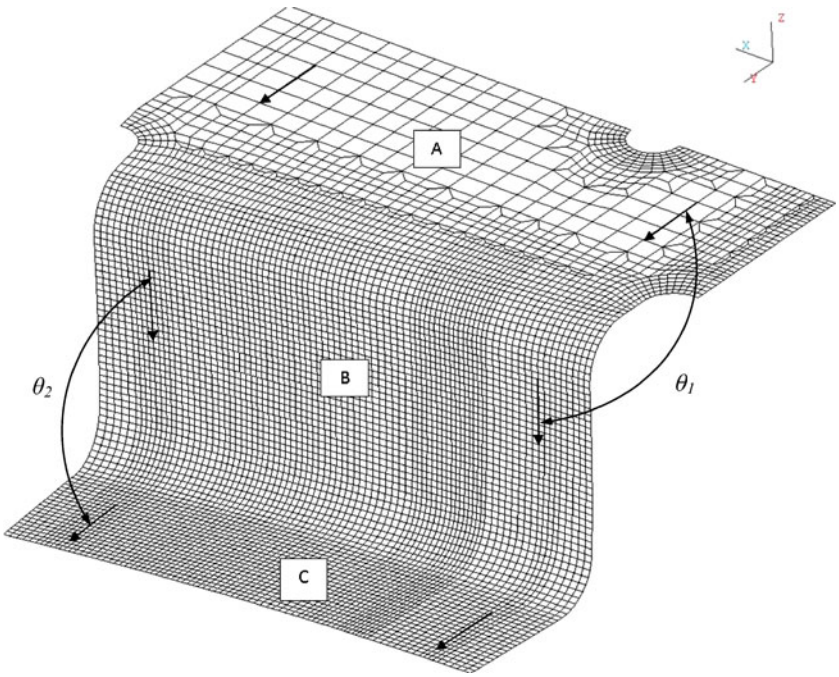

Fig. 3 Springback angle measurement procedure

$$\begin{aligned} &find \quad R_d, R_p \\ &\min \quad w_1 \frac{\mu_{(\theta_1+\theta_2)}(R_d,R_p)}{\mu_{(\bar{\theta}_1+\bar{\theta}_2)}} + w_2 \frac{\sigma_{(\theta_1+\theta_2)}(R_d,R_p)}{\sigma_{(\bar{\theta}_1+\bar{\theta}_2)}} \\ &s.t \quad R_d^L \le R_d \le R_d^U \\ &\quad R_p^L \le R_p \le R_p^U \end{aligned} \tag{4}$$

where R_d^L, R_p^L, R_d^U, and R_p^U are the lower and upper bounds of R_d and R_p, respectively. μ and σ refer to the mean and standard deviation, $\bar{\theta}_1$, $\bar{\theta}_2$, and $\bar{\theta}_1 + \bar{\theta}_2$ are the nominal values for θ_1, θ_2, and $\theta_1 + \theta_2$, respectively. In (2–4), both the mean and the standard deviation of springback $\left(\mu_{\theta_1}, \sigma_{\theta_1}, \mu_{\theta_2}, \sigma_{\theta_2}, \mu_{\theta_1+\theta_2}, \text{ and } \sigma_{\theta_1+\theta_2}\right)$ are minimized. The weighting factors w_1 and w_2 are chosen based on the importance of reducing the mean and the standard deviation of springback and also satisfy $w_1 + w_2 = 1$. For example, if minimizing the mean value of springback is more important than minimizing the standard deviation, the weighting factors are selected as $w_1 > w_2$.

Overall, 19 different optimization cases are considered for all flanges and the optimization problems defined in this section are solved by using "*fmincon*" built-in function of MATLAB® (2009) that uses sequential quadratic programming. To increase the probability of finding the global optimum, a multiple starting point strategy is used.

3 Finite element simulations

Accuracy and precision of the FEA results depends on how the physical process parameters are simulated. Moreover, some numerical and mathematical parameters as contact algorithm, number of integration points, element size, element formulation and material model affect the accuracy of the results (Lin et al. 2000). Yield locus of the material is determined by using 3-paramater Barlat material model in accordance with anisotropic behavior of the blank. The true plastic stress- true plastic strain curve of the material is determined according to Swift's hardening rule given in (5).

$$\sigma = K\left(\varepsilon_0 + \varepsilon^p\right)^n \tag{5}$$

Here, σ is the true plastic stress, K is the hardening exponent, ε_0 is the initial strain corresponding to yield stress, ε^p is the true plastic strain and n is the hardening exponent. Material properties of the DP600 steel used in experiments are given in Table 2.

Forming simulations can be carried out by using explicit or implicit formulations (Prior 1994). Explicit formulation reduces the computation time, however, it leads to convergence problems. It can be overcome by choosing the proper numerical parameters, i.e., die velocity. The use of the real value of the die velocity in finite element (FE) simulations results in huge computational cost. On the other hand, the value of the die velocity should not exceed a critical value in order to avoid inertial effects. In this study, die velocity is taken as 2,000 mm/s in FE simulations.

The finite element model of the blank is constructed with 79,932 deformable quadrilateral shell elements. It is required to use fine elements for high deformation regions and around radii of the part to eliminate the hourglass effect. Consequently, minimum element size of the quadrilateral elements is determined as 0.5 mm × 0.5 mm. Fully integrated shell element formulation is used for the deformable blank and Belytschko-Tsay element formulation is used for rigid parts. The punch, the die and the holder are modeled as rigid and relatively coarser elements are used. Eleven elements are used through the shoulder radii of the punch and the die. "ONE_WAY_SURFACE_TO_SURFACE" contact algorithm is used for the contact definitions. To eliminate contact instabilities, contact stiffness parameter, SLDFAC set as 0.01. The static and dynamic friction coefficients are taken as 0.125 and 0.06, respectively.

Seven integration points have been used to differentiate the stress distribution through the thickness of the blank in according to 0.8 mm blank thickness. For the given physical and numerical parameters, the computation time is 8 h and 13 min with Xeon X5550 2.67 GHz 16 CPU. When 15 integration points have been used the computation time is increased to 24 h 37 min.

The FEA results are compared with experimental results. The experiments are conducted at COŞKUNÖZ METAL FORM Company facilities. A hydraulic driven press equipped with 200 tons is used. The velocity of the die averages 30 mm/s. Two slots are equipped to the punch to simplify blank positioning and to increase the repeat accuracy. The experiments are conducted for 40 DP 600 steel blanks which were cut from the same batch. The tensile test specimens are also acquired from the same plate. Blanks are located as the rolling direction passes through the Flange #1 and Flange #4. Only a single experiment is conducted. Outer surfaces of the formed part are scanned using ATOS 3D Scanning Software and Systems (see Fig. 4).

Table 2 Material properties of the DP600 steel

	K(MPa)	n	ε_0	σ_Y (MPa)	E (GPa)	υ	R_0	R_{45}	R_{90}
DP600	1207.8	0.222	0.006509	395	210	0.3	0.70	0.70	0.86

Fig. 4 The experimental springback measurements using ATOS 3D Scanning Software and Systems

The comparison of the FEA results and the experimental results are given in Table 3. The difference between the two sets of results can be evaluated by considering the accuracy of both sets of results. As noted earlier, the experimental springback measurements are performed using ATOS 3D Scanning Software and Systems. The following procedure is employed while computing the springback angle from the measurements of the experimental data. First, surfaces are created from the scanned data obtained from ATOS 3D. Then, a measurement procedure similar to the one followed in the case of finite element analysis is applied. A total of eight points are required for each flange, except Flange #6 for which only four points are needed. The measured values depend on the points chosen in the measurement process (see Fig. 3). So, there is uncertainty associated with the measured values. In addition, there is uncertainty in the finite element results. Note here that the random variables also reflect uncertainty in the properties of the specimens used in experiments to compare with finite element models. The standard deviation of the springback (borrowed from the future Tables 10, 11 and 29) may provide a coarse estimation. There is also the uncertainty associated with the difference between the test article and the geometry of the modeled article. Also, due to the nonuniformity in material properties, the material properties of the test article and the modeled article can be quite different. The absolute errors of nine out of 13 predictions are smaller than or equal to 1 degree, and in the light of the above discussions the difference can be considered reasonable.

4 Surrogate modeling techniques

The approximation models for highly complicated and expensive FEA can be constructed using surrogate models. The surrogate models create a functional relationship between design variables (e.g., punch and die radius) and responses (e.g., springback). Thus, usual engineering practices such as design space exploration, sensitivity analysis and design optimization become practical. Construction of a surrogate model begins with choosing a design of experiment (DoE) for creating sampling data, then continues with selecting a mathematical model to represent the data, and ends with determining the best fitting model to the sampling data (accuracy of the surrogate models).

Two sets of surrogate models are constructed in this study. The first set is constructed to relate the springback to the design variables as well as random variables. The mean and the standard deviation of springback are calculated using MCS, where the first set of surrogate models is utilized. The second set of surrogate models is generated to relate the mean and the standard deviation of springback to the design variables.

It must be noted that the problem can be solved without generating a second set of surrogate models. The main reason for using the second set of surrogate models is to eliminate the noise induced by the Monte Carlo simulation. Therefore, the second set of surrogate models helps in convergence of the gradient-based optimizer used in this work.

Table 3 Comparison of the FEA results and experimental results of springback angles in degrees

# Flange	Experiments (Ave.)		LS-DYNA		Errors	
	θ_1	θ_2	θ_1	θ_2	θ_1	θ_2
1	0.0	1.0	0.6 (0.2)[a]	1.8 (0.3)	0.6	0.8
2	10.3	6.2	6.4 (0.6)	5.2 (0.2)	−3.9	−1
3	9.7	4.3	7.6 (0.6)	6.4 (0.4)	−2.1	2.1
4	0.9	3.2	0.6 (0.1)	4.2 (0.5)	−0.3	1
5	5.7	3.9	3.7 (0.3)	4.3 (0.4)	−2	0.4
6	10.4	–	9.8 (0.0)	–	−0.6	–
7	5.5	6.0	5.0 (0.4)	6.5 (0.3)	−0.5	0.5

[a]The standard deviation values are borrowed from Tables 10, 11, and 29

If a second set of surrogate models is not to be generated, then the MCS sample size can be increased to reduce the MCS noise and this slight noise can be handled by using a global optimizer (e.g., genetic algorithm, particle swarm optimization, etc.).

4.1 Data sampling (set #1)

Among the DoE techniques, Latin hypercube sampling (LHS) technique (Park 1994) is used to iteratively generate samples to maximize minimum distance between sampling points. This method is employed by using "*lhsdesign*" built-in function of MATLAB® (2009) and "*maximin*" criterion with a maximum of 20 iterations. 65 sampling points are created for different material properties, die and punch radii and the springback values (θ_1, θ_1) at these points are computed using LS-DYNA for each flange. The minimum and maximum values for process variables are provided in Table 4.

In this study, all flanges are considered simultaneously, because our preliminary investigations revealed that the design variables for a specific flange do not affect the springback of the other flanges. For Flanges #1, #4 and #6 there are eight variables (one design variable and seven random variables), whereas for the remaining flanges there are nine variables (two design variable and seven random variables). The use of 65 training points for 9 variables is not impressive, but it is not unreasonable either. A quadratic response surface approximation with all terms included has 55 coefficients for 9 variables. So the additional 10 points helps to find these coefficients in least square sense. It must be noted that the rule of thumb advocates the use of 90 training points, but we had to settle for 65 points as the simulations are very expensive as explained in the followings.

For any of the 65 training points, springback calculation requires performing the followings: (a) geometry generation (around 1.5 h), (b) mesh generation (around 1.5 h), (c) LS-DYNA model generation (around 0.5 h), (d) LS-DYNA problem solving (around 8.5 h), (e) LS-DYNA post-processing of the springback values (around 1 h). The overall time spent for a single training point is approximately 13 h. All these simulations are performed by a single graduate student mostly using a single computer.

The sampling domains of the input random variables affect the prediction accuracies of the mean and the standard deviation of the output, and there are tradeoffs of accuracy. If a narrow sampling domain of input random variables is chosen, then the surrogate models would be more accurate but there is a larger chance that the surrogate model would perform extrapolation in MCS, and the extrapolation is dangerous. On the other hand, if a wide sampling domain of input random variables is chosen, then the surrogate models would be less accurate but there is a smaller chance that the surrogate model would perform extrapolation in MCS. In this work, we started with mean +/−5*sigma domain and found that the surrogate models were accurate enough, so we did not need to shrink the domain.

Before generating the surrogate models, a simple sensitivity analysis is performed to investigate the effects of design and random variables on springback. The details of the sensitivity analysis are provided in Appendix A. It is found that the punch radius is more influential than the die radius for θ_1, whereas the opposite is true for θ_2. Among the random variables, the hardening coefficient and the hardening exponent are found to be the most influential variables. It is also observed that the anisotropy coefficient R_{90} has more influence on springback compared to the other anisotropy coefficients R_0 and R_{45}.

4.2 Surrogate models (set #1)

The next step, following the selection of DoE type, is the computation of the springback values at the training points using LS-DYNA. After performing these simulations, the observed data which contains springback values is used together with the DoE information to construct surrogate models. In this study, four different surrogate types with seven different models are considered: namely, PRS (PRS1, first-order and PRS2, second-order), SWR (SWR1, first-order and SWR2, second order), RBF (multiquadric model) and KR (KR0, zeroth-order and KR1, first-order trend model). For a brief overview of these surrogate models,

Table 4 Minimum and maximum values for process variables

Variable	Design variables (different for each flange)											Random variables (same for all flanges)						
	F#1	F#2		F#3		F#4	F#5		F#6	F#7								
	R_p^*	R_d^*	R_p	R_d	R_p	R_p	R_d	R_p	R_p	R_d	R_p	σ_Y^{**}	K^{**}	n	R_0	R_{45}	R_{90}	RD^a
Min.	2	3	3	3	3	4	3	3	3	3	3	230	950	0.140	0.7	0.7	0.8	0
Max.	4	10	10	10	10	6	10	10	12	10	10	430	1210	0.222	1.1	1.2	1.4	1

*R_p and R_d values are in mm, **σ_Y and K values are in MPa, [a]RD stands for "Rolling Direction" (y = 0, x = 1)

the reader should refer to Appendix B of Acar et al. (2011). Then, these constructed surrogate models are used for performing robust optimization. Finally, for each flange the optimum values of the design variables, predicted by surrogate models, are validated using MCS. In this study, a surrogate-based robust optimization procedure is pursued. Figure 5 depicts the flowchart for robust optimization of the flanges.

In this study, we are satisfied with the accuracy of surrogate models built with 65 training points at the first stage, and the accuracy of surrogate models built with 20 training points at the second stage. Therefore, it was not required to add points to the DOE (see Fig. 5). If we had not satisfied with the accuracy of the surrogate models, the new points could have been added by following the EGO strategy proposed by Jones et al. (1998) such that the expected improvement is maximized.

4.3 Accuracy of the surrogate models (set #1)

As noted earlier, PRS1, PRS2, SWR1, SWR2, RBF, KR0 and KR1 surrogate models are constructed for θ_1 and θ_2 prediction. The accuracy of the constructed surrogate models for each flange is assessed using the root mean square

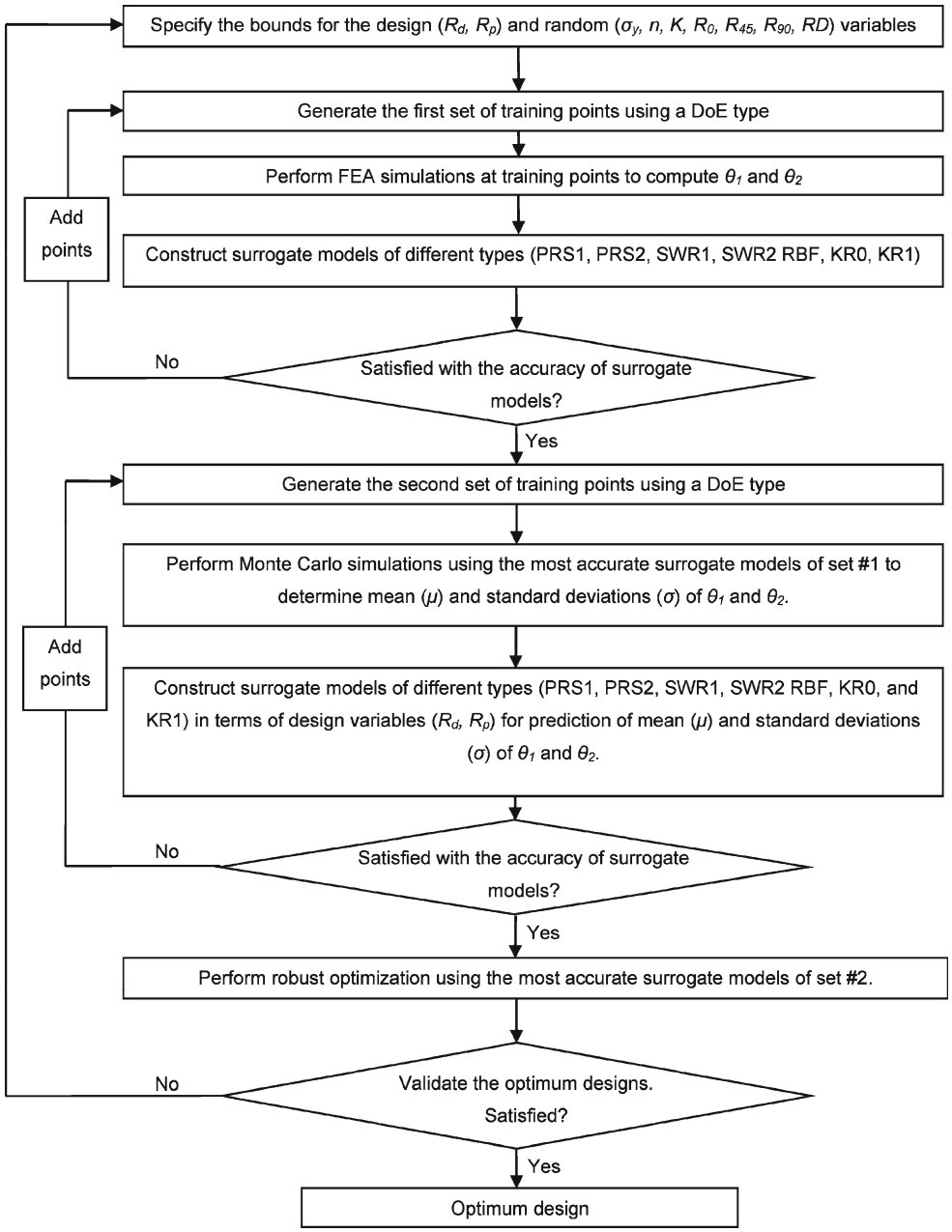

Fig. 5 Flowchart for performing surrogate-based robust optimization of the seven-flange die assembly

Table 5 The most accurate surrogate models of set #1 for each flange

Flange #	Prediction model for θ_1	Prediction model for θ_2
1	SWR1	PRS1
2	RBF	KR1
3	RBF	KR1
4	SWR1	SWR1
5	KR1	KR1
6	KR0	—
7	RBF	KR1

of the leave-one-out cross validation error ($RMSE_{XV}$). To calculate the $RMSE_{XV}$, first a surrogate model type is constructed N times (where N is the number of training points), while leaving out one of the training points as the validation data each time. Then $RMSE_{XV}$ value is obtained using (6).

$$RMSE_{XV} = \sqrt{\frac{1}{N}\sum_{i=1}^{N}\left(y_i - \hat{y}_{(i)}\right)^2} \tag{6}$$

where y_i is the observed value at the retained training point x_i, and $\hat{y}_{(i)}$ is the predicted value. Then, $RMSE_{XV}$ is normalized with the range of observed values Δy (8).

$$\Delta y = y_{\max} - y_{\min} \tag{7}$$

$$\varepsilon = (RMSE_{XV}/\Delta y) \times 100 \tag{8}$$

where y_{max} and y_{min} are the maximum and minimum value of the observed data among the 65 training points, respectively. The most accurate surrogate models of set #1 for each flange are listed in Table 5. It is observed that KR models are more accurate than PRS, SWR and RBF for most of the cases. The accuracy evaluation of the surrogate models constructed for θ_1 and θ_2 of Flange #1 is provided in Table 6. The accuracy evaluation of the surrogate models of the other flanges are given in Appendix B. Note here that if the finite element analysis was computationally inexpensive, it would be better to evaluate the accuracy of the surrogate models at some test points.

Table 7 Statistical properties of the random variables. Normal distribution parameters for random variables

Continuous random variables (all are normally distributed)		
Variable	Mean	Standard deviation
σ_y[MPa]	330	20
n	0.1810	0.0082
K [MPa]	1080	26
R_0	0.90	0.04
R_{45}	0.95	0.05
R_{90}	1.10	0.06
Discrete random variables		
RD	= 0 with 50% probability	
	= 1 with 50% probability	

5 Optimization methodology

The optimization procedure, described in Fig. 5, is used to select the optimal values of the design variables. The upper and lower bounds of the design variables R_d *and* R_p were provided earlier in Table 4. The random variables (σ_Y, n, K, R_0, R_{45} and R_{90}) are assumed to be normally distributed and the distribution parameters are provided in Table 7. The rolling direction RD is a discrete random variable represented with a probability mass function. This variable is also taken into account in MCS.

Notice that the mean values of the material properties in Table 7 do not coincide with the material properties listed in Table 2. The material properties listed in Table 2 correspond to the particular batch from which the specimens are prepared. The mean and standard deviation of the material properties in Table 7 is obtained from all available DP600 data the COŞKUNÖZ METAL FORM Company have. The difference between the mean values in Tables 7 and 2 reflects the batch-to-batch variability in material properties.

Table 6 Accuracies of different surrogate models constructed for θ_1 and θ_2 (Flange #1)

	PRS1	PRS2	SWR1	SWR2	RBF	KR0	KR1
Accuracies of surrogate models for θ_1 prediction ***RMSE/Δy (%)***	11.3	17.5	**11.2**	21.7	13.8	23.8	11.5
R^2	0.80	0.52	0.80	0.26	0.70	0.11	0.79
Accuracies of surrogate models for θ_2 prediction ***RMSE/Δy (%)***	**7.6**	10.8	7.9	18.3	8.6	11.9	7.7
R^2	**0.82**	0.63	0.81	−0.05	0.76	0.55	0.81

5.1 Surrogate models (set #2)

To compute the $\mu_{\theta_1}, \sigma_{\theta_1}, \mu_{\theta_2}, \sigma_{\theta_2}, \mu_{\theta_1+\theta_2}$, and $\sigma_{\theta_1+\theta_2}$ values in (2–4), the most accurate surrogate models of the first set are embedded into MCS (10,000 samples). Then, a second set of surrogate models is constructed to relate $\mu_{\theta_1}, \sigma_{\theta_1}, \mu_{\theta_2}$, and σ_{θ_2} to the design variables. For that purpose, a new set of training points (10 times the number of variables) is generated using LHS. For each training point, MCS with 10,000 samples is performed, where 10,000 different values are selected for each random variable using their normal distribution parameters. It is assumed that all random variables are uncorrelated, and this assumption may lead to over prediction of the springback variation. The springback values θ_1 and θ_2 are computed 10,000 times for each training point and the mean and standard deviation of θ_1 and θ_2 are evaluated. Finally, the second set of surrogate models are constructed for $\mu_{\theta_1}, \sigma_{\theta_1}, \mu_{\theta_2}$, and σ_{θ_2} in terms of design variables.

The accuracy of the mean and the standard deviation computed through MCS can be assessed by the standard error estimations of these statistics. The standard error of the mean can be estimated from $\frac{\sigma}{\sqrt{N}}$, while the standard error of the standard deviation can be estimated from $\sigma\sqrt{\frac{1}{2}\left(1-\sqrt{\frac{N-3}{N-1}}\right)}$ assuming that the sample is drawn from a normal distribution. Here σ is the standard deviation and N is the number of samples in MCS. With 10,000 samples, the standard error of the mean is 0.01 σ and the standard error of the standard deviation is 0.0071 σ. So, the accuracies of the mean and the standard deviation will be dictated by the accuracy of the surrogate models.

5.2 Accuracy of the surrogate models (set #2)

The ratio of $RMSE_{XV}$ to the range of response values (Δy) and the R^2 values are used to select the most accurate surrogate models (out of the second set of surrogate models) for each response. The most accurate surrogate model types for all flanges are listed in Table 8. It is seen that PRS models are more accurate than SWR, KR and RBF models for most of the cases. The accuracies of the second set of surrogate models in terms of R^2 values are given in Table 9. The R^2 values of the surrogate models in set#2 constructed for the mean springback values are larger than the corresponding surrogate models in set #1. The R^2 values of the surrogate models in set#2 constructed for the standard deviation of the springback values, on the other hand, are not that impressive.

Table 8 The most accurate surrogate model of set #2 for each flange

Flange #	μ_{θ_1}	σ_{θ_1}	μ_{θ_2}	σ_{θ_2}
1	PRS2	PRS1	PRS2	PRS1
2	PRS2	SWR1	PRS1	KR0
3	KR0	PRS2	PRS1	PRS1
4	PRS1	PRS2	KR1	PRS1
5	KR1	SWR2	KR0	PRS2
6	PRS1	PRS1	—	—
7	RBF	SWR1	KR0	KR0

Table 9 The accuracy of the second set of surrogate models in terms of R^2 values

Flange ID	μ_{θ_1}	μ_{θ_2}	σ_{θ_1}	σ_{θ_2}
1	1.00	0.01	0.99	0.47
2	0.99	0.94	1.00	0.04
3	0.98	0.82	0.97	0.39
4	1.00	0.49	0.99	0.01
5	0.99	0.22	0.98	0.28
6	0.18	0.11	—	—
7	0.98	0.38	0.94	0.08

After the surrogate models are generated for μ_{θ_1}, σ_{θ_1}, μ_{θ_2}, and σ_{θ_2}, the values of $\mu_{\theta_1+\theta_2}$ and $\sigma_{\theta_1+\theta_2}$ are approximated in terms of μ_{θ_1}, σ_{θ_1}, μ_{θ_2}, and σ_{θ_2} using the Taylor series expansion as

$$\mu_{\theta_1+\theta_2} \cong \mu_{\theta_1} + \mu_{\theta_2} \tag{9}$$

$$\sigma_{\theta_1+\theta_2} \cong \sqrt{\sigma_{\theta_1}^2 + \sigma_{\theta_2}^2} \tag{10}$$

Equations (9) and (10) are valid if θ_1 and θ_2 have a weak correlation and the higher order terms in the Taylor series expansion are negligible.

6 Optimization results

In this section, the optimum results for the seven flanges are provided. Totally 19 optimization cases are considered for optimization of θ_1, θ_2, $\theta_1 + \theta_2$. We do not have a strong preference for reducing the mean or the standard deviation,

Table 10 Coefficients of the PRS models for θ_1, and θ_2 for Flange #1

	θ_1		θ_2	
	μ	σ	μ	σ
Constant	0.83576	0.17261	2.09130	0.32097
R_p	0.74096	−0.00109	1.21400	0.00187
R_p^2	−0.09226	—	−0.14480	—

Table 11 Optimization results for Flange #1. ($w_1 = w_2 = 0.5$)

	θ_1			θ_2			$\theta_1 + \theta_2$		
	Nominal (actual)	Optim. (pred.)	Optim. (actual)	Nominal (actual)	Optim. (pred.)	Optim. (actual)	Nominal (actual)	Optim. (pred.)	Optim. (actual)
μ	2.227	1.949	1.952	4.436	3.940	3.903	6.663	5.889	5.854
σ	0.173	0.170	0.173	0.336	0.325	0.326	0.377	0.367	0.369
R_d	–	–	–	–	–	–	–	–	–
R_p	3.0	2.0	2.0	3.0	2.0	2.0	3.0	2.0	2.0

so the weight factors in (2–4) are taken as $w_1 = w_2 = 0.5$. The optimum results are obtained using the second set of surrogate models (in terms of design variables). Then, MCS of the optimum designs are carried out to validate the prediction accuracy of the surrogate models.

6.1 Flange #1

For Flange #1, die (R_d) and punch (R_p) radii are dependent, so only R_p is used as design variable. R_p is the input variable for the surrogate models to predict θ_1, and θ_2 values. The lower and the upper bounds of the input variable are specified as 2 mm $\leq R_p \leq$ 4 mm. PRS2 is used for μ_{θ_1} and μ_{θ_2} prediction while PRS1 is used for σ_{θ_1} and σ_{θ_2} prediction (see Table 8). Table 10 lists the coefficients of the PRS models for θ_1, and θ_2 of Flange #1. Note that a PRS model in terms of R_p has the following form;

$$\text{PRS1} = \text{Constant} + \text{Coeff}^* R_p \tag{11}$$

$$\text{PRS2} = \text{Constant} + \text{Coeff}_1{}^* R_p + \text{Coeff}_2{}^* R_p^2 \tag{12}$$

Robust optimization for θ_1 is performed using the surrogate models (PRS models) with the coefficients provided in Table 10 (columns 2 and 3). As noted earlier, the weight factors for the mean and the standard deviation of springback are taken equal in robust optimization. That is, equal importance has been given to minimize the mean springback and standard deviation of springback. Table 11 presents a comparison of the mean and the standard deviation of springback for the nominal design (column 2) and the optimum design (both the surrogate model prediction (column 3) as well as the MCS validation (column 4) at the found optimum). If the surrogate model predictions did not involve errors, we could conclude that the mean springback could be reduced by about 12.5% and the standard deviation of springback could be reduced by 2%. Due to the errors in surrogate model predictions, on the other hand, the mean springback is reduced by about 12.3% and the standard deviation of springback is maintained at its nominal value. The optimum value of the punch radius R_p is found to be 2 mm, which is the lower bound of R_p.

Then, robust optimization for θ_2 is performed using PRS models with the coefficients provided in Table 10 (columns 4 and 5). Optimum results for μ_{θ_2}, σ_{θ_2} and R_p are listed in Table 11 (columns 5 to 7). It is observed that the mean springback is reduced by about 12% and the standard deviation of springback is reduced by about 3%. The optimum value of the punch radius R_p is found to be 2 mm, as in the case of θ_1 minimization.

Finally, the optimization results for $\theta_1 + \theta_2$ are presented in Table 11 (columns 8 to 10). It is found that the mean springback is reduced by about 12% and the standard deviation of springback is reduced by about 2%. The optimum value of the punch radius R_p is found to be 2 mm, as in the case of θ_1 and θ_2 minimization.

6.2 Flange #2

For Flange #2, die (R_d) and punch (R_p) radii are independent, so both R_d and R_p are used as design variables. R_d and R_p are the input variables for the surrogate models to predict θ_1 and θ_2 values. The lower and upper bounds of the input

Table 12 Optimization results for Flange #2 ($w_1 = w_2 = 0.5$)

	θ_1			θ_2			$\theta_1 + \theta_2$		
	Nominal (actual)	Optim. (pred.)	Optim. (actual)	Nominal (actual)	Optim. (pred.)	Optim. (actual)	Nominal (actual)	Optim. (pred.)	Optim. (actual)
μ	4.260	1.754	2.286	6.015	1.535	1.581	10.276	5.321	5.457
σ	0.630	0.479	0.498	0.175	0.179	0.186	0.654	0.511	0.474
R_d	6.5	3.0	3.0	6.5	10.0	10.0	6.5	10.0	10.0
R_p	6.5	10.0	10.0	6.5	10.0	10.0	6.5	10.0	10.0

Table 13 Design variables and their lower (LB) and upper bounds (UB) for Flanges #3 through #7

	Flange #3		Flange#4	Flange #5		Flange #6	Flange #7	
	R_d	R_p	R_p	R_d	R_p	R_p	R_d	R_p
LB	3	3	4	3	3	3	3	3
UB	10	10	6	10	10	12	10	10

variables specified as 3 mm $\leq R_d \leq$ 10 mm, and 3 mm $\leq R_p \leq$ 10 mm, respectively. PRS2 is used for μ_{θ_1} prediction while SWR1 is used for σ_{θ_1} prediction. For μ_{θ_2} and σ_{θ_2} prediction, PRS1 and KR0 are used.

Then, robust optimization for θ_1 is performed, where the weight factors for the mean and the standard deviation of springback are taken equal, as in the case of Flange #1. Table 12 presents a comparison of the mean and the standard deviation of springback for the nominal design (column 2) and the optimum design (both the surrogate model prediction (column 3) as well as the MCS validation (column 4) at the found optimum). The mean springback is reduced by about 46.3% and the standard deviation of springback could be reduced by 21%. The optimum value of the die radius R_d is found to be 3 mm, which is the lower bound of R_d. The optimum value of the punch radius R_p is found to be 10 mm, which is the upper bound of R_p.

Then, robust optimization for θ_2 is performed using PRS1 and KR0 models. Optimum results for $\mu_{\theta_2}, \sigma_{\theta_2}, R_d$ and R_p are listed in Table 12 (columns 5 to 7). It is observed that the mean springback is reduced by about 73.7% and the standard deviation of springback is increased by about 6.3%. The optimum value of the die radius R_d is found to be 10 mm, which is the upper bound of R_d. The optimum value of the punch radius R_p is found to be 10 mm, as in the case of θ_1 minimization.

Finally, the optimization results for $\theta_1 + \theta_2$ are presented in Table 12 (columns 8 to 10). It is found that the mean springback is reduced by about 47% and the standard deviation of springback is reduced by about 27.5%. The optimum values of the die (R_d) and punch (R_p) radii are found to be 10 mm, as in the case of θ_1 and θ_2 minimization.

6.3 Flanges #3 through #7

For Flanges #3 through #7, design variables and their lower and upper bounds are listed in Table 13. Table 14 presents the optimization results for θ_1, θ_2, and $\theta_1 + \theta_2$ of Flanges #3 through #7.

Robust optimizations for θ_1 of Flanges #3 through #7 are performed using the surrogate models listed in Table 8. The weight factors for the mean value and the standard deviation of springback are taken equal for robust optimization cases of all flanges, as in the case of Flange #1 and #2. The optimum results for Flange #3 through #7 are provided in Appendix C. Overall, mean springback values $\left(\mu_{\theta_1}, \mu_{\theta_2}\right)$ are reduced in amounts varying between 7% and 85% compared to nominal mean springback values. Standard deviation of springback values are reduced slightly for some cases, significantly for some other cases compared nominal standard deviation of springback values. It should be also noted that the standard deviation of springback values are increased slightly for some cases, too.

The optimum die and punch radius results for all flanges are compiled together in Table 14. It can be concluded that upper and lower bounds of the die and punch radii are influential for most cases. For Flanges #1 through #4 optimum die and punch radii are observed at upper or lower bounds. On the other hand, optimization studies for Flanges #5 and #7 showed that all of the optimum die radius values are found at between upper and lower bounds of their own. Besides, optimum punch radius values are mostly found at their upper bounds (except for θ_2 minimization). In addition, determining the lower bound for punch radius is critical for θ_1 minimization of Flange #6.

Table 14 Optimum die radius and punch radius results for all flanges ($w_1 = w_2 = 0.5$). It is indicated with (LB) or (UB) whenever a design variable takes the lower or upper bound

Minimization for	Flange #1	Flange #2	Flange #3	Flange #4	Flange #5	Flange #6	Flange #7
Optimum die radius							
θ_1	—	3.0 (LB)	3.0 (LB)	—	9.53	—	8.45
θ_2	—	10.0 (UB)	10.0 (UB)	—	8.75	—	8.38
$\theta_1 + \theta_2$	—	10.0 (UB)	10.0 (UB)	—	9.53	—	8.45
Optimum punch radius							
θ_1	2.0 (LB)	10.0 (UB)	7.52	6.0 (UB)	10.0 (UB)	3.0 (LB)	10.0 (UB)
θ_2	2.0 (LB)	10.0 (UB)	10.0 (UB)	4.0 (LB)	7.55	—	4.04
$\theta_1 + \theta_2$	2.0 (LB)	10.0 (UB)	10.0 (UB)	6.0 (UB)	10.0 (UB)	—	10.0 (UB)

Table 15 Optimization results obtained using nine combinations of multiple surrogates

			$\theta_2(w_1 = w_2 = 0.5)$[°]								
		Stage 1	KR1[a]			RTF			KPR2		
		Stage 2	KR0[a]	PRS1	SWR2	KR0	PRS1	SWR2	KR0	PRS1	SWR2
		Nom.	Opt #1	Opt #2	Opt #3	Opt #4	Opt #5	Opt #6	Opt #7	Opt #8	Opt #9
Flange #5	μ	5.677	3.443	3.144	1.142	3.190	2.929	2.074	3.948	3.383	3.227
	σ	0.371	0.410	0.289	0.379	0.281	0.177	0.458	1.174	0.800	1.222
	R_d	6.50	8.75	10.00	10.00	9.97	10.00	10.00	9.33	10.00	10.00
	R_p	6.50	7.55	3.00	5.19	4.43	3.00	3.26	4.76	3.00	4.43

[a]the most accurate surrogate models at the first and the second stages are KR1 and KR0, respectively

The general observations obtained from optimization results can be described as follows. Two different types of beading are investigated. Flange #1 has continuous beading through the web, whereas in Flange #4 the beads are applied at the radii of the flanges. Flange #4 shows the best mean performance as well as the smallest springback variation. So, this design is the most robust design. It can be concluded that introducing beads increases the mean performance and the robustness. Flange #2 and #3 (concave and convex, respectively) showed the worst mean performances as well as the largest springback variation. Even though the concave and convex flanges improved the aerodynamic characteristics and the appearance, they result in significant springback and variation. It is observed that a design change that decreases the mean springback also reduces the springback variation. That is, the deterministic design and the robust design are similar.

6.4 Using multiple surrogates

As pointed out by Glaz et al. (2009) and later by Acar et al. (2011), in a surrogate based optimization framework, the use of the most accurate surrogate model does not necessarily lead to the optimum. In this section, instead of using the most accurate surrogate model in optimization, the use of multiple surrogates is explored. Since there exist two sets of surrogate models in this work, the use of multiple surrogates is a bit problematic. Recall that we use seven different surrogate models in each set, so there exist 49 possible combinations of multiple surrogates, and it becomes a tedious work. To simplify the analysis, we use the surrogate models with the best, the average and the worst performance. In addition, out of 19 optimization problems considered for the seven-flange die assembly, we focus on θ_2 minimization Flange #5, because for this optimization problem the design variables take optimal values within the bounds. In most of the other cases out of 19 optimization problems, the design variables are pushed to the lower or upper bounds.

For θ_2 minimization of Flange #5, the surrogate models with the best, the average and the worst performance are KR1, RBF and SWR2, respectively, among the first set of surrogates. When, KR1 model is used in the first stage, the surrogate models with the best, the average and the worst performance are KR0, PRS1 and SWR2, respectively, among the second set of surrogates. So we consider these multiple surrogate models at two stages, and solve the robust optimization problem using nine combinations of these models. The optimization results obtained using nine combinations of multiple surrogates are provided in

Table 16 Performance evaluation of candidate optimum designs using multiple surrogates

	Candidate optimum	R_d [mm]	R_p [mm]	$\theta_2(w_1 = w_2 = 0.5)$ [°]			Ave. [°]
				KR0	PRS1	SWR2	
KR1	#1	8.75	7.55	3.443	4.075	2.735	3.417
	#2	10.00	3.00	5.320	3.144	1.387	3.284
	#3	10.00	5.19	4.673	3.154	1.142	2.990
RBF	#4	9.97	4.43	3.190	3.041	2.205	2.812
	#5	10.00	3.00	3.359	2.929	2.063	2.784
	#6	10.00	3.26	3.314	2.946	2.074	**2.778**
SWR2	#7	9.33	4.76	3.948	4.141	3.779	3.956
	#8	10.00	3.00	4.362	3.383	3.492	3.746
	#9	10.00	4.43	4.094	3.496	3.227	3.605

Table 17 Optimum die radius and punch radius results for all flanges obtained by using a single set of surrogate models ($w_1 = w_2 = 0.5$)

Minimization for	Flange #1	Flange #2	Flange #3	Flange #4	Flange #5	Flange #6	Flange #7
Optimum die radius							
θ_1	—	3.0 (LB)	3.0 (LB)	—	7.05	—	10.0 (UB)
θ_2	—	10.0 (UB)	10.0 (UB)	—	9.42	—	8.57
$\theta_1 + \theta_2$	—	10.0 (UB)	10.0 (UB)	—	7.45	—	10.0 (UB)
Optimum punch radius							
θ_1	2.0 (LB)	10.0 (UB)	7.99	6.0 (UB)	10.0 (UB)	3.0 (LB)	10.0 (UB)
θ_2	2.0 (LB)	10.0 (UB)	10.0 (UB)	4.0 (LB)	4.48	—	5.47
$\theta_1 + \theta_2$	2.0 (LB)	10.0 (UB)	10.0 (UB)	6.0 (UB)	10.0 (UB)	—	10.0 (UB)

Table 15. We consider all these designs as candidate optimum designs. It is observed that the candidate optimum designs #2, #5 and #8 are identical, so the use of multiple surrogates leads to seven different candidate optimum configurations.

The last step of surrogate-based optimization is the validation of the optimum designs. For a deterministic optimization problem, it requires performing a single finite element analysis. For a robust optimization problem, the validation will require performing many finite element analyses within a Monte Carlo framework. In this study, there exist two layers of surrogate models in robust optimization, so the validation of optimum is also problematic. First of all, it is computationally very expensive to evaluate the actual performances of the candidate optimum designs that require direct integration of finite element analysis into a Monte Carlo simulation framework. As a remedy, the performances of the candidate optimum designs are predicted using multiple surrogates and the average performance of the candidate optimum over multiple surrogates is assessed. Table 16 shows that the average performance of the candidate #6 over multiple surrogates is better than that of the candidate #1, which corresponds to the use of the most accurate surrogate models at each stage. This result underlines the fact that in surrogate-based optimization, the use of multiple surrogates is a better strategy than using the most accurate surrogate model in optimization.

6.5 Comparing the use of two sets of surrogates to a single set of surrogate

One may argue that the use of the second set of surrogate models built upon the first set of surrogate models increases the overall error and leads to erroneous optimization results. To investigate this issue of inaccuracy associated with the second set of surrogates, the optimization problems are also solved by using the first set of surrogates within an MCS framework. To deal with the MCS noise, the set of random variables are generated only once at the beginning and the same random variables are used throughout the optimization.

The optimization results obtained by using a single set of surrogate models are provided in Tables 17 and 18. Comparing the optimal values of the design variables given in Table 17 to the results in Table 13, it is seen that the optimal values of the design variables obtained using a single set of surrogate models and two sets of surrogate models are close. Similarly, comparing the optimal springback values in Table 18 to the results in Tables 10, 11 and 29, it is observed that the values obtained using a single set of surrogate models and two sets of surrogate models are close.

Table 18 Optimum springback results for all flanges obtained by using a single set of surrogate models ($w_1 = w_2 = 0.5$)

Minimization for	Flange #1	Flange #2	Flange #3	Flange #4	Flange #5	Flange #6	Flange #7
Mean values							
θ_1	1.952	2.286	3.798	0.606	0.332	1.458	1.394
θ_2	3.903	1.581	3.465	4.869	4.245	—	1.642
$\theta_1 + \theta_2$	5.854	5.457	9.022	5.475	4.088	—	4.597
Standard deviations							
θ_1	0.173	0.498	0.701	0.087	0.262	0.00004	0.348
θ_2	0.326	0.186	0.630	0.470	0.313	—	0.189
$\theta_1 + \theta_2$	0.369	0.474	0.737	0.478	0.531	—	0.435

7 Conclusion

In this paper, robust optimization of DP600 steel seven-flange die assembly was performed. The design variables were selected as the die radius and the punch radius. The random variables of the problem were the yield stress, the hardening exponent, the hardening coefficient, the anisotropy coefficients and the rolling direction. Mean and standard deviation of the springback values were optimized using surrogate models. Two sets of surrogate models were constructed in this study. The first set was constructed to relate the springback to the design variables as well as the random variables. The mean and the standard deviation of springback were calculated using MCS, where the first set of surrogate models was utilized. The second set of surrogate models was generated to relate the mean and the standard deviation of springback to the design variables. From the results obtained, the following conclusions were drawn:

- Two different types of beading are investigated. Flange #1 has continuous beading through the web, while the beads are applied at the radii of Flange #4. Flange #4 showed the best mean performance as well as the smallest springback variation. So, this design was the most robust design. From the springback results obtained, it was concluded that introducing beads increased both the mean performance and the robustness.
- Flange #2 and #3 (concave and convex, respectively) showed the worst mean performances as well as the largest springback variation. Even though the concave and convex flanges may improve the aerodynamic characteristics and the appearance, they result in significant springback and variation.
- Four different types of surrogate models were utilized, namely PRS (PRS1, PRS2), SWR (SWR1, SWR2), RBF and KR (KR0, KR1). It was found for the first set of surrogate models that KR provided more accurate springback predictions than PRS, SWR and RBF. It was found for the second set of surrogate models that PRS provided more accurate springback predictions than SWR, RBF and KR.
- The surrogate based robust optimization was performed and MCS were performed to validate the found optimum. Considerable reductions were obtained for the mean values of different springback angles in amounts varying between 7% and 85% when compared to nominal mean springback results.
- It is observed that a design change that decreases the mean springback also reduces the springback variation. That is, the deterministic design and the robust design are similar.
- The standard deviation was not significantly changed for the optimal design, and the small number of design variables was responsible for this outcome. Increasing the number of design variables could help reducing the standard deviation of the springback.
- Since the springback of each flange in the seven-flange die assembly required individual treatment, nineteen different optimization problems were formulated and it was observed for most cases that the optimizer pushed the design variables to lower and upper bounds.
- The use of multiple surrogates in optimization was evaluated and it was observed that finding multiple candidates of optimum with multiple surrogates and selecting the one with the best performance is a better strategy than optimization with the most accurate surrogate model.

Acknowledgments The authors greatly acknowledge the support provided by COŞKUNÖZ METAL FORM for sharing the experimental facilities, and thank Mustafa Yenice and Mesut Kaya of COŞKUNÖZ METAL FORM for their help in the experiments. Also, the financial support provided by the Scientific and Technological Research Council of Turkey (TÜBİTAK), under award MAG-109M078, is greatly acknowledged.

Appendix A: Sensitivity analysis

To investigate the effects of design and random variables on springback, a simple sensitivity analysis is performed. The variables as well as the springback values are normalized between 0 and 1. A linear PRS is fitted to the normalized springback in terms of normalized variables. The coefficients of the linear terms are indications of the sensitivity of springback to the variables. The coefficients are listed in Table 19 for θ_1 and in Table 20 for θ_2. The absolute values of the coefficients are listed in descending order in Table 21 for θ_1 and in Table 22 for θ_2. It is found that the punch radius is more influential than the die radius for θ_1, whereas the opposite is true for θ_2. Among the random variables, the hardening coefficient and the hardening exponent are found to be the most influential variables. Finally, the anisotropy coefficient R_{90} is observed to have more influence than the other anisotropy coefficients R_0 and R_{45}.

Appendix B: Accuracy evaluation of the surrogate models of Flanges #2 through #7

The accuracy evaluation of the surrogate models of Flange #2 through #7 are listed in Tables 23, 24, 25, 26, 27, 28. SWR models show the best performance for Flange #4 θ_1 and θ_2. RBF model is the most accurate model for Flange #2 θ_1, Flange #3 θ_1, and Flange #7 θ_1. Kriging models show

Table 19 The sensitivity of θ_1 to the design variables and the random variables

Variable	Flange #1	Flange #2	Flange #3	Flange #4	Flange #5	Flange #6	Flange #7
R_d		0.278	0.323		−0.137		−0.133
R_p	0.136	−0.329	−0.372	−0.417	−0.516	−0.216	−0.506
σ_Y	0.148	−0.005	−0.016	0.037	0.042	0.163	0.047
N	−0.285	−0.248	−0.243	−0.046	−0.249	−0.169	−0.211
K	0.268	0.349	0.323	0.171	0.113	−0.157	0.237
R_0	−0.065	−0.106	−0.089	−0.051	−0.084	−0.059	−0.123
R_{45}	0.046	0.007	−0.025	0.017	0.089	0.083	0.031
R_{90}	0.141	0.188	0.146	0.072	0.106	0.278	0.152
RD	−0.053	0.091	0.068	−0.107	0.075	0.015	0.033

Table 20 The sensitivity of θ_2 to the design variables and the random variables

Variable	Flange #1	Flange #2	Flange #3	Flange #4	Flange #5	Flange #7
R_d		−0.756	−0.354		−0.552	−0.585
R_p	0.145	−0.289	−0.189	0.076	−0.041	0.096
σ_Y	−0.130	−0.022	−0.075	−0.152	−0.051	0.050
N	−0.255	−0.037	−0.152	−0.452	−0.131	−0.105
K	0.294	0.111	0.116	0.360	0.240	0.244
R_0	−0.028	−0.002	−0.053	−0.051	0.019	−0.101
R_{45}	0.015	0.029	−0.044	0.002	−0.025	0.001
R_{90}	0.084	0.074	0.066	0.105	0.151	−0.011
RD	−0.046	−0.021	0.077	−0.060	0.053	0.030

Table 21 The sorted listings of the sensitivity of θ_1 to the design variables and the random variables

Variable	Flange #1	Flange #2	Flange #3	Flange #4	Flange #5	Flange #6	Flange #7
R_d		3	3		3		5
R_p	5	2	1	1	1	2	1
σ_Y	3	9	9	7	9	4	7
N	1	4	4	6	2	3	3
K	2	1	2	2	4	5	2
R_0	6	6	6	5	7	7	6
R_{45}	8	8	8	8	6	6	9
R_{90}	4	5	5	4	5	1	4
RD	7	7	7	3	8	8	8

Table 22 The sorted listings of the sensitivity of θ_2 to the design variables and the random variables

Variable	Flange #1	Flange #2	Flange #3	Flange #4	Flange #5	Flange #7
R_d		1	1		1	1
R_p	3	2	2	5	7	5
σ_Y	4	7	6	3	6	6
N	2	5	3	1	4	3
K	1	3	4	2	2	2
R_0	7	9	8	7	9	4
R_{45}	8	6	9	8	8	9
R_{90}	5	4	7	4	3	8
RD	6	8	5	6	5	7

Table 23 Accuracies of different surrogate models constructed for θ_1 and θ_2 (Flange #2)

	PRS1	PRS2	SWR1	SWR2	RBF	KR0	KR1
Accuracies of surrogate models for θ_1 prediction ***RMSE/*Δ*y (%)***	5.5	8.2	5.3	12.7	**4.9**	15.8	5.5
R^2	0.92	0.82	0.92	0.57	0.94	0.33	0.92
Accuracies of surrogate models for θ_2 prediction ***RMSE/*Δ*y (%)***	8.9	28.3	9.6	47.0	9.6	26.3	**8.9**
R^2	0.89	−0.14	0.87	−2.14	0.87	0.02	0.89

Table 24 Accuracies of different surrogate models constructed for θ_1 and θ_2 (Flange #3)

	PRS1	PRS2	SWR1	SWR2	RBF	KR0	KR1
Accuracies of surrogate models for θ_1 prediction ***RMSE/*Δ*y (%)***	7.2	11.4	7.5	15.3	**6.7**	16.0	7.0
R^2	0.88	0.71	0.87	0.48	**0.90**	0.43	0.89
Accuracies of surrogate models for θ_2 prediction ***RMSE/*Δ*y (%)***	8.9	17.4	8.9	23.1	9.0	12.5	**7.5**
R^2	0.72	−0.08	0.72	−0.88	0.71	0.45	**0.80**

Table 25 Accuracies of different surrogate models constructed for θ_1 and θ_2 (Flange #4)

	PRS1	PRS2	SWR1	SWR2	RBF	KR0	KR1
Accuracies of surrogate models for θ_1 prediction ***RMSE/*Δ*y (%)***	14.2	22.6	**14.2**	33.3	21.3	21.0	14.8
R^2	0.43	−0.44	**0.44**	−2.11	−0.27	−0.24	0.39
Accuracies of surrogate models for θ_2 prediction ***RMSE/*Δ*y (%)***	7.2	12.2	**7.1**	14.4	8.3	13.8	7.2
R^2	0.85	0.56	**0.85**	0.38	0.79	0.43	0.84

Table 26 Accuracies of different surrogate models constructed for θ_1 and θ_2 (Flange #5)

	PRS1	PRS2	SWR1	SWR2	RBF	KR0	KR1
Accuracies of surrogate models for θ_1 prediction ***RMSE/*Δ*y (%)***	18.6	51.6	19.4	58.7	18.7	24.1	**18.4**
R^2	0.53	−2.64	0.49	−3.72	0.52	0.21	**0.54**
Accuracies of surrogate models for θ_2 prediction ***RMSE/*Δ*y (%)***	11.3	23.3	11.5	28.4	11.7	15.6	**10.6**
R^2	0.69	−0.31	0.68	−0.94	0.67	0.41	**0.73**

Table 27 Accuracies of different surrogate models constructed for θ_1 and θ_2 (Flange #6)

	PRS1	PRS2	SWR1	SWR2	RBF	KR0	KR1
Accuracies of surrogate models for θ_1 prediction ***RMSE/*Δ*y (%)***	28.6	52.9	28.2	77.8	44.4	**28.0**	28.7
R^2	−0.08	−2.68	−0.05	−6.97	−1.60	−0.03	−0.08

Table 28 Accuracies of different surrogate models constructed for θ_1 and θ_2 (Flange #7)

	PRS1	PRS2	SWR1	SWR2	RBF	KR0	KR1
Accuracies of surrogate models for θ_1 prediction ***RMSE/*Δ*y (%)***	16.4	28.5	16.9	37.1	**16.3**	19.8	16.4
R^2	0.49	−0.53	0.46	−1.61	**0.50**	0.26	0.49
Accuracies of surrogate models for θ_2 prediction ***RMSE/*Δ*y (%)***	12.6	18.7	13.7	34.4	14.0	14.0	**10.8**
R^2	0.60	0.13	0.53	−1.95	0.51	0.51	**0.71**

the best performance for Flange #2 θ_2, Flange #3 θ_2, Flange #5 θ_1 and θ_2, Flange #6 θ_1, Flange #7 θ_2. PRS models do not show superiority over other surrogate models for any of the responses.

Appendix C: Optimization results for Flanges #2 through #7

Table 29 presents a comparison of the mean and the standard deviation of springback for the nominal design (column 2, 3, and 9) and the optimum design (both the surrogate model prediction (column 4, 7, and 10) as well as the MCS results (column 5, 8, 11) at the found optimum).

For θ_1 minimization of Flange #3, optimum results are provided in Table 29 (rows 3 to 6, columns 3 to 5). The mean springback is reduced by 39% and the standard deviation of the springback is increased by about 16.4%. The optimum values of the die and punch radii are found to be 3 mm (lower bound of R_d) and 7.52 mm, respectively. For θ_2 minimization of Flange #3, optimum results are presented in Table 29 (rows 3 to 6, columns 6 to 8). It is observed that the mean springback is reduced by 49.5% and the standard deviation of the springback is increased by about 71.2%. The optimum values of the die and punch radii are both found to be 10 mm (upper bound of R_d and R_p). For $\theta_1 + \theta_2$ minimization of Flange #3, optimum results are listed in Table 29 (rows 3 to 6, columns 9 to 11). It is found that

Table 29 Optimization results for Flanges #3 through #7 ($w_1 = w_2 = 0.5$)

		θ_1			θ_2			$\theta_1 + \theta_2$		
		Nominal results	Optim. (pred.)	Optim. (actual)	Nominal results	Optim. (pred.)	Optim. (actual)	Nominal results	Optim. (pred.)	Optim. (actual)
Flange #3	μ	6.544	4.492	3.984	6.582	2.995	3.465	13.402	8.873	9.233
	σ	0.616	0.644	0.717	0.638	0.245	0.630	0.718	0.355	0.746
	R_d	6.50	3.00	3.00	6.50	10.00	10.00	6.50	10.00	10.00
	R_p	6.50	7.52	7.52	6.50	10.00	10.00	6.50	10.00	10.00
Flange #4	μ	0.934	0.611	0.606	5.258	4.825	4.869	6.192	5.977	5.475
	σ	0.087	0.088	0.087	0.481	0.475	0.470	0.489	0.475	0.478
	R_d	–	–	–	–	–	–	–	–	–
	R_p	5.00	6.00	6.00	5.00	4.00	4.00	5.00	6.00	6.00
Flange #5	μ	2.475	0.388	0.355	5.677	3.443	4.831	8.152	4.155	3.931
	σ	0.257	0.705	0.280	0.371	0.410	0.348	0.451	0.992	0.630
	R_d	6.50	9.53	9.53	6.50	8.75	8.75	6.50	9.53	9.53
	R_p	6.50	10.00	10.00	6.50	7.55	7.55	6.50	10.00	10.00
Flange #6	μ	1.458	1.458	1.458	–	–	–	–	–	–
	σ	0.00290	0.00001	0.00004	–	–	–	–	–	–
	R_d	–	–	–	–	–	–	–	–	–
	R_p	7.50	3.00	3.00	–	–	–	–	–	–
Flange #7	μ	3.815	1.716	1.593	3.692	1.378	1.573	7.507	5.127	4.794
	σ	0.349	0.356	0.383	0.266	0.326	0.234	0.439	0.473	0.493
	R_d	6.50	8.45	8.45	6.50	8.38	8.38	6.50	8.45	8.45
	R_p	6.50	10.00	10.00	6.50	4.04	4.04	6.50	10.00	10.00

the mean springback is reduced by 31.1% and the standard deviation of the springback is increased by about 4%. The optimum values of the die and punch radii are both found to be 10 mm (upper bound of R_d and R_p), as in the case of θ_2 minimization.

For θ_1 minimization of Flange #4, optimum results are provided in Table 29 (rows 7 to 10, columns 3 to 5). The mean springback is reduced by 35.1% and the standard deviation of springback is maintained at its nominal value. The optimum value of the punch radius is found to be 6 mm, which is the lower bound of R_p. For θ_2 minimization of Flange #4, optimum results are presented in Table 29 (rows 7 to 10, columns 6 to 8). It is observed that the mean springback is reduced by 7.4% and the standard deviation of the springback is decreased by about 2.3%. The optimum value of the punch radius is found to be 4 mm. For $\theta_1 + \theta_2$ minimization of Flange #4, optimum results are listed in Table 29 (rows 7 to 10, columns 9 to 11). It is found that the mean springback is reduced by 11.6% and the standard deviation of the springback is decreased by about 2.3%. The optimum value of the punch radius is found to be 6 mm (upper bound of R_p), as in the case of θ_1 minimization.

For θ_1 minimization of Flange #5, optimum results are provided in Table 29 (rows 11 to 14, columns 3 to 5). The mean springback is reduced by 85.7% and the standard deviation of the springback is increased by about 9%. The optimum values of the die and punch radii are found to be 9.53 mm and 10 mm (upper bound of R_p), respectively. For θ_2 minimization of Flange #5, optimum results are presented in Table 29 (rows 11 to 14, columns 6 to 8). It is observed that the mean springback is reduced by 14.9% and the standard deviation of the springback is reduced by about 7.6%. The optimum values of the die and punch radii are found to be 8.75 mm and 7.55 mm, respectively. For $\theta_1 + \theta_2$ minimization of Flange #5, optimum results are listed in Table 29 (rows 11 to 14, columns 9 to 11). It is found that the mean springback is reduced by 51.8% and the standard deviation of the springback is increased by about 39.7%. The optimum values of the die and punch radii are found to be 9.53 mm and 10 mm (upper bound of R_p), respectively, as in the case of θ_1 minimization.

For θ_1 minimization of Flange #6, optimum results are provided in Table 29 (rows 15 to 18, columns 3 to 5). The mean springback is maintained at its nominal value and the standard deviation of springback is reduced by about 98.6%. The optimum value of the punch radius is found to be 3 mm, which is the lower bound of R_p.

For θ_1 minimization of Flange #7, optimum results are provided in Table 29 (rows 19 to 22, columns 3 to 5). The mean springback is reduced by 58.2% and the standard deviation of the springback is increased by about 9.7%. The optimum values of the die and punch radii are found to be 8.45 mm and 10 mm (upper bound of R_p), respectively. For θ_2 minimization of Flange #7, optimum results are presented in Table 29 (rows 19 to 22, columns 6 to 8). It is observed that the mean springback is reduced by 57.4% and the standard deviation of the springback is reduced by about 12%. The optimum values of the die and punch radii are found to be 8.38 mm and 4.04 mm, respectively. For $\theta_1 + \theta_2$ minimization of Flange #7, optimum results are listed in Table 29 (rows 19 to 22, columns 9 to 11). It is found that the mean springback is reduced by 36.1% and the standard deviation of the springback is increased by about 12.3%. The optimum values of the die and punch radii are found to be 8.45 mm and 10 mm (upper bound of R_p), respectively, as in the case of θ_1 minimization.

As noted earlier, we assumed that the weight coefficients are equal ($w_1 = w_2 = 0.5$). Predicted and actual optimum result will change with values of the w_1 and w_2. For example, if μ_{θ_1} is more important than σ_{θ_1}, then we would use $w_1 > w_2$ in optimization and we would obtain a smaller μ_{θ_1} value than the μ_{θ_1} value presented in Table 11. However, there is a trade-off. If w_1 is larger than the w_2, the σ_{θ_1} will be larger than the σ_{θ_1} value evaluated at equal weight coefficients ($w_1 = w_2 = 0.5$). That is, determining the weight coefficients is up to designer. Designer's performance expectation from a system is important to decide whether w_1 must be larger than w_2 or not. The same assessment can be made for the results of Flanges #2 through #7.

References

Acar E, Guler MA, Gerçeker B, Cerit ME, Bayram B (2011) Multi-objective crashworthiness optimization of tapered thin-walled tubes with axisymmetric indentations. Thin-Walled Struct 49(1):94–105

Buhmann MD (2003) Radial basis functions: theory and implementations. Cambridge University Press, New York

Chen P, Koc M (2007) Simulation of springback variation in forming of advanced high strength steels. J Mater Process Technol 190:189–198

de Souza T, Rolfe BF (2010) Characterizing material and process variation effects on springback robustness for a semi-cylindrical sheet metal forming process. Int J Mech Sci 52:1756–1766

Du X, Venigella PK, Liu D (2009) Robust mechanism synthesis with random and interval variables. Mech Mach Theory 44:1321–1337

Finn MJ, Galbraith PC, Wu L, Hallquist JO, Lum L, Lin TL (1995) Use of a coupled explicit-implicit solver for calculating springback in automotive body panels. J Mater Process Technol 50:395–409

Glaz B, Goel T, Liu L, Friedmann PP, Haftka RT (2009) Multiple-Surrogate approach to helicopter rotor blade vibration reduction. AIAA J 47(1):271–282

Ingarao G, Di Lorenzo R, Micari F (2009) Analysis of stamping performances of dual phase steels: a multi-objective approach to reduce springback and thinning failure. Mater Des 30:4421–4433

Jones DR, Schonlau M, Welch WJ (1998) Efficient global optimization of expensive black-box functions. J Glob Optim 13:455–492

Li YQ, Cui ZS, Ruan XY, Zhang DJ (2005) Application of six sigma robust optimization in sheet metal forming. AIP Conf Proc 778:819–824

Liew K, Tan H, Ray T, Tan M (2004) Optimal process design of sheet metal forming for minimum springback via integrated neural network evolutionary algorithm. Struct Multidisc Optim 26:284–294

Lin Z, Liu G, Xu W, Bao Y (2000) Study on the effects of numerical parameters on the precision of springback prediction. In: Proceedings of the sixth international LS-DYNA users conference 5

Lophaven SN, Nielsen HB, Søndergaard J (2002) DACE-a MATLAB kriging toolbox, informatics and mathematical modeling. Technical University of Denmark, Lyngby

Marretta L, Ingarao G, Di Lorenzo R (2010) Design of sheet stamping operations to control springback and thinning: a multi-objective stochastic optimization approach. Int J Mech Sci 52:914–927

MATLAB® (2009) User's guide and reference guide

Meinders T, Burchitz IA, Bonte MHA, Lingbeek RA (2008) Numerical product design: springback prediction, compensation and optimization, Int. J Mach Tools Manuf 48:499–514

Myers RH, Montgomery DC (2002) Response surface methodology: process and product optimization using designed experiments. Wiley, New York

Naceur H, Guo YQ, Ben-Elechi S (2006) Response surface methodology for design of sheet forming parameters to control springback effects. Comput Struct 84:1651–1663

Naceur H, Ben-Elechi S, Batoz JL, Kropf-Lenoir C (2008) Response surface methodology for the rapid design of aluminum sheet metal forming parameters. Mater Des 29:781–790

Park JS (1994) Optimal Latin-hypercube designs for computer experiments. J Stat Plan Inference 39:95–111

Prior AM (1994) Applications of implicit and explicit finite element techniques to metal forming. J Mater Process Technol 45: 649–656

Sacks J, Welch WJ, Mitchell TJ, Wynn HP (1989) Design and analysis of computer experiments. Stat Sci 4(4):409–435

Strano M (2008) A technique for FEM optimization under reliability constraint of process variables in sheet metal forming. Int J Mater Form 1:13–20

Wang W, Hou B, Lin Z, Xia ZC (2009) An Engineering approach to improve the stamping robustness of high strength steels. J Manuf Sci Eng 131:1–5

Wei L, Yuying Y, Zhongwen X, Lihong Z (2009) Springback control of sheet metal forming based on the response-surface method and multi-objective genetic algorithm. Mater Sci Eng 499:325–328

Zhang W, Shivpuri R (2008) Investigating reliability of variable blank holder force control in sheet drawing under process uncertainties. J Manuf Sci E-T ASME. doi:10.1115/1.2951936